AN ANALYTICAL STUDY OF THE DILATION OF FAST REACTOR FUEL ASSEMBLY DUCTS

D. P. CHAN, R. J. JACKSON

Reference Fuel Department, Westinghouse Hanford Company, Richland, Washington 99352, U.S.A.

SUMMARY

To ascertain that a fast reactor fuel assembly duct will meet its design life, one of the technical issues to be examined is the duct-to-duct touching due to duct dilations. With the availability of finite element computer programs, the duct dilation problem can be easily analyzed. However, because of the variation of pressure, temperature, and fast neutron flux throughout the reactor core, the number of cases to be analyzed for different combinations of loading conditions is very large. A fast analytical method is introduced to solve the two-dimensional duct dilation problem. Assuming symmetry conditions in geometry and loading, one-sixth of the duct cross-section (one flat) is analyzed. The method calculates the stress, strain and dilation of the duct wall in time increments. The loads (temperature, pressure differential, and fast neutron flux) and the stress distribution are assumed constant within each time increment. As long as the creep strain is linearly dependent on the stress, the formulation and solution of the dilation problem are exactly those for an elastic analysis with the addition of irradiation creep and swelling terms in the stress-strain relationship. The moment at any time step is related not only to the curvature at that time step (as in an elastic analysis), but also to all the moments at the previous time steps. Knowing the moment, shear and displacement at time zero, the corresponding results at subsequent times can be determined by "marching on" the solution. Solutions are carried out for two cases: 1) a duct with constant pressure differential, 2) a duct with varying pressure differential. Results are in close agreement with finite element results of the MARC-CDC program. The computer running time for the method is one or two orders of magnitude less than that for the finite element program. The method is used to predict the dilation of the Fast Test Reactor ducts in different core positions. Quantitative results are obtained indicating, 1) the maximum dilation occurs at the mid-flat of the duct, 2) the maximum stress and accumulated inelastic strain occur at the inside corner of the duct, 3) dilation decreases with thickness and increases with duct size, 4) dilation increases with temperature, internal pressure, fast neutron flux and irradiation time. On the basis of a parametric study covering all the extreme loading conditions of the FTR core, it is concluded that, for the material laws assumed, the FTR ducts will not touch each other due to dilation alone in their intended length of service.

1. INTRODUCTION

In the Fast Test Reactor (FTR) core, there are 73 driver fuel assemblies. The principal structural members of a fuel assembly are the fuel pin bundle and the duct tube. Most assemblies are designed to operate in the FTR core for 300 full power days. To ascertain that the duct tube will meet its design life, several technical issues have to be examined, one of which is the dilation of the duct under pressure, temperature and fast neutron fluence. The duct wall must be thick enough so that 1) there is not enough dilation of the ducts to cause duct-to-duct touching, and 2) there is not enough accumulated total inelastic strain in the duct to cause duct failure. Conversely, the ducts must be as thin as practical to reduce the amount of metal in the core, which captures neutrons and thus impairs the breeding performance of the reactor. In the following, for temperatures <755K (900°F) where creep is linearly dependent on stress, an analytic method is introduced, which can easily calculate the stress, strain and deflection of the duct wall as a function of its irradiation history.

2. THEORY

For a hexagonal duct under internal pressure, uniform temperature and fast neutron flux, a two-dimensional mathematical model of 1/6 of the duct is shown in Figure 1, where symmetry conditions in geometry and loading are assumed. The basic equations are:

Equilibrium

$$p_n = \frac{dV_n}{dx} \tag{1}$$

$$V_n = \frac{dM_n}{dx} - F_n \frac{dw_n}{dx} \tag{2}$$

Compatibility

$$\varepsilon_n = -z \frac{d^2 w_n}{dx^2} + \frac{du_n}{dx} \tag{3}$$

Stress-Strain

$$\varepsilon_n = \frac{\sigma_n}{E} + \alpha T_n + \sum_{i=o}^{n-1} \Delta\varepsilon_i^s + \sum_{i=o}^{n-1} \Delta\varepsilon_i^c \tag{4}$$

where

$$\Delta\varepsilon_n^c = \sigma_n \tilde{K}_n \phi_n \Delta t_n \tag{5}$$

$$\Delta\varepsilon_n^s = R_n \phi_n \Delta t_n \tag{6}$$

$\tilde{K}(\phi t, T)$ and $R(\phi t, T)$ are functions of fast neutron fluence and temperature.

By substituting equ. (3) into equ. (4), multiplying both sides of the resulting equation by the distance to the centroid, and integrating over the cross-sectional area of the duct wall, the following equation is obtained:

$$M_n = E\left[-I\frac{d^2 w_n}{dx^2} - \sum_{i=o}^{n-1} K_i M_i\right] \tag{7}$$

where $K_i = \tilde{K}_i \phi_i \Delta t_i$

Equ. (7) indicates that the moment at any time step n is related to the curvature at time step n and all the moments at the previous time steps. The moment can be expressed as:

$$M_n = a_o^n \frac{d^2 w_n}{dx^2} + a_1^n \frac{d^2 w_{n-1}}{dx^2} + \dots a_n^n \frac{d^2 w_o}{dx^2} \tag{8}$$

where $a_o^n = -EI$

$a_1^n = E^2 \; I \; K_{n-1}$

$a_2^n = E^2 \; I \; K_{n-2} \; (1-K_{n-1}E)$

$\vdots$

$a_n^n = E^2 \; I \; K_o \; (1-K_1E)(1-K_2E) \; . \; . \; . \; (1-K_{n-1}E)$

By substituting equ. (8) into equ. (2), the shear at any time can be expressed as:

$$V_n = a_o^n \frac{d^3 w_n}{dx^3} + a_1^n \frac{d^3 w_{n-1}}{dx^3} + \; . \; . \; . \; + a_n^n \frac{d^3 w_o}{dx^3} - F_n \frac{dw_n}{dx} \tag{9}$$

From equs. (1) and (9), the governing equation of the duct dilation problem is:

$$p_n = a_o^n \frac{d^4 w_n}{dx^4} + a_1^n \frac{d^4 w_{n-1}}{dx^4} + \; . \; . \; . \; a_n^n \frac{d^4 w_o}{dx^4} - F_n \frac{d^2 w_n}{dx^2} \tag{10}$$

Nondimensionalizing according to the following,

$\bar{w}_n = \frac{w_n}{h}$, $\bar{F}_n = \frac{F_n h}{EL^2}$,

$\bar{u}_n = \frac{Lu_n}{h^2}$, $\bar{V}_n = \frac{V_n}{EL}$,

$\bar{x} = \frac{x}{L}$, $\bar{M}_n = \frac{M_n}{Eh^2}$,

$\beta = \frac{h}{L}$, $\bar{p}_n = \frac{p_n}{E}$,

the governing equation can be expressed as:

$$\bar{p}_n = -\frac{\beta^4}{12} \frac{d^4 \bar{w}_n}{d\bar{x}^4} + \frac{K_{n-1}E\beta^4}{12} \frac{d^4 \bar{w}_{n-1}}{d\bar{x}^4} + \frac{K_{n-2}(1-K_{n-1}E) \; E\beta^4}{12} \frac{d^4 \bar{w}_{n-2}}{d\bar{x}^4}$$

$$+ \; . \; . \; . \; + \frac{K_o(1-K_1E)(1-K_2E) \; . \; . \; . (1-K_{n-1}E) \; E\beta^4}{12} \frac{d^4 \bar{w}_o}{d\bar{x}^4} - \bar{F}_n \frac{d^2 \bar{w}_n}{d\bar{x}^2} \tag{11}$$

The associated boundary conditions are

$$\frac{d\overline{w}_n}{d\overline{x}}(0) = 0 \tag{12}$$

$$\overline{V}_n(0) = 0 \tag{13}$$

$$\frac{d\overline{w}_n}{d\overline{x}}(1) = 0 \tag{14}$$

$$\cos 30^\circ \, \beta \, \overline{u}_n(1) + \sin 30^\circ \, \overline{w}_n(1) = 0 \tag{15}$$

Equs. (12) and (14) state that the slopes are zero at the end points. Equ. (13) states that the shear is zero in the middle of the duct wall. Equ. (15) states that the displacement in the z' direction, Fig. 1, is zero. All four equations stem from the fact that the boundaries have symmetry conditions.

The solution to equ. (11) for varying p_n is:

$$\overline{w}_n = C_1^n \overline{x} + C_2^n + C_3^n e^{\gamma_1^n \overline{x}} + C_4^n e^{\gamma_2^n \overline{x}} - \frac{\overline{p}_n}{2\overline{F}_n} \overline{x}^2 + C_5^n e^{\gamma_1^{n-1} \overline{x}}$$

$$+ C_6^n e^{\gamma_2^{n-1} \overline{x}} + C_7^n e^{\gamma_1^{n-2} \overline{x}} + C_8^n e^{\gamma_2^{n-2} \overline{x}} + \ldots + C_{2n+3}^n e^{\gamma_1^0 \overline{x}}$$

$$+ C_{2n+4}^n e^{\gamma_2^0 \overline{x}} \tag{16}$$

where the first four terms on the right-hand-side constitute the homogeneous solution, and the remaining terms, the particular solution. The roots of the homogeneous solution and the undetermined parameters of the particular solution can be found as follows:

Substituting the homogeneous solution into equ. (11) yields,

$$\left.\begin{aligned} \gamma_1^n &= \sqrt{\frac{-12\overline{F}_n}{\beta^4}}\,, \\ \gamma_2^n &= \gamma_1^n \quad . \end{aligned}\right\} \tag{17}$$

Substituting the particular solution into equ. (11) yields,

$$C_5^n = \frac{\dfrac{K_{n-1}E\beta^4}{12} C_3^{n-1} \left(\gamma_1^{n-1}\right)^2}{\dfrac{\beta^4}{12}\left(\gamma_2^{n-1}\right)^2 + \overline{F}_n}$$

$$C_6^n = \frac{\dfrac{K_{n-1}E\beta^4}{12} C_4^{n-1} \left(\gamma_2^{n-1}\right)^2}{\dfrac{\beta^4}{12}\left(\gamma_2^{n-1}\right)^2 + \overline{F}_n}$$

$$C_7^n = \frac{\frac{K_{n-2}(1-K_{n-1}E)E\beta^4}{12} C_3^{n-2} \left(\gamma_1^{n-2}\right)^2 + \frac{K_{n-1}E\beta^4}{12} C_5^{n-1} \left(\gamma_1^{n-2}\right)^2}{\frac{\beta^4}{12}\left(\gamma_1^{n-2}\right)^2 + \overline{F}_n}$$

$$C_8^n = \frac{\frac{K_{n-2}(1-K_{n-1}E)E\beta^4}{12} C_4^{n-2} \left(\gamma_2^{n-2}\right)^2 + \frac{K_{n-1}E\beta^4}{12} C_6^{n-1} \left(\gamma_2^{n-2}\right)^2}{\frac{\beta^4}{12}\left(\gamma_2^{n-2}\right)^2 + \overline{F}_n}$$

$$\vdots \qquad (18)$$

On the basis of equilibrium for 1/6th of the duct wall, it can be shown that $\overline{F}_n = -2 \cos 30\ \beta\ \overline{p}_n$. With the present and past γ's and $\overline{F}$'s known, C_5, C_6, ... C_{2n+3}, C_{2n+4} can be determined.

The solution $\overline{w}_n$ is left with 4 unknowns, C_1^n, C_2^n, C_3^n, and C_4^n. There are 4 boundary conditions available, namely, equs. (12), (13), (14), and (15). Substituting $\overline{w}_n$ into the boundary conditions yields a system of simultaneous algebraic equations, by which C_1^n, C_2^n, C_3^n and C_4^n can be solved.

With w_n known, shear can be determined from equ. (9), and moment from equ. (8). Stress and strain can be determined as follows:

$$\sigma_n = E\left(\frac{\overline{F}_n}{\beta^2} + 6\overline{M}_n\right)$$

$$\varepsilon^s = \sum_{i=o}^{n-1} R_i \phi_i \Delta t_i$$

$$\varepsilon^c = \sum_{i=o}^{n-1}\left(\frac{\overline{F}_i}{\beta^2} + 6\overline{M}i\right) EK_i$$

As will be shown in the results section, the bending moment is fairly constant with time for the case of constant internal pressure. Assuming that the moment is constant, equ. (7) reduces to:

$$M_n = \frac{-I}{\frac{1}{E} + \sum_{i=o}^{n-1} K_i} \frac{d^2 w_n}{dx^2} \qquad (19)$$

The solution of the above equation is the same as the elastic solution with the exception of the irradiation creep term in the denominator.

A computer program "DUCT" was written incorporating the equations developed in this section to calculate the stress, strain and deflection values of the duct under irradiation.

In the following, stress, strain and deflection results by the DUCT program are presented for 1) the case of constant internal pressure using equ. (19), and 2) the case of

varying internal pressure using equation (8). The results are compared to the finite element results of the MARC-CDC program, [1].

3. RESULTS

In row one at the midplane of the FTR core, the following conditions exist on the duct wall during steady state operation at a nominal coolant inlet temperature of 633K (680°F):

1) temperature of 741K (875°F)
2) pressure differential of 0.22 MPa (32 psi)
3) neutron flux of 4.5×10^{15} n/cm^2-sec (E > 0.1 Mev)

The duct tube is .30 cm (.120 inch) in thickness and 11.62 cm (4.575 inches) across outside flats. The material is 316 stainless steel with 20% cold work. At 741K (875°F), thermal creep can be neglected. The irradiation creep law and the irradiation swelling law of Gilbert [2] and Bates [3] were used in the analysis.

Figure 2 describes the dilations of the duct wall at the beginning-of-life and at the end of 3 operating cycles (7200 hrs). The maximum dilation occurs at the mid-flat, and the minimum, at the corner. At the beginning-of-life, the duct wall is under constant temperature and pressure. At the end-of-irradiation, the duct wall is under the same temperature and pressure, but with the addition of fast neutron fluence. The difference of the dilation curves at the beginning-of-life and at the end-of-irradiation corresponds to the permanent deformation in the duct wall when it is depressurized and brought to room temperature following irradiation.

Figure 3 describes the bending stress along the inside surface of the duct wall at the beginning-of-life and at the end-of-irradiation. The bending stress is compressive at the mid-flat, and tensile at the corner. Maximum stress occurs at the corner. At the end-of-irradiation there is very little stress relaxation. As an approximation, stresses can be assumed constant with time.

Figure 4 describes the accumulated creep strain along the inside surface of the duct wall at the end-of-irradiation. Because of the high bending stress at the duct corner, the accumulated creep strain is maximum there.

To check the accuracy of the DUCT results, a finite element model of 1/12th of the duct wall was established. Three two-dimensional isoparametric curved beam elements of the MARC-CDC program were used. The large displacement option was used. Dilation, stress and strain predictions are shown as dotted curves in Figures 2, 3, and 4. The dotted curves are very close to the solid curves obtained from the DUCT program.

Another case was analyzed assuming the same temperature and flux as before but with varying internal pressure. A pressure of .22 MPa (32 psi) was used for 1-1/2 cycles of operation (3600 hrs). It was then increased linearly to .44 MPa (64 psi) by the end of the third cycle (7200 hrs) due to a hypothetical fuel bundle and duct interaction. Table 1 compares the corner stress, accumulated corner strain, and maximum duct dilation as calculated by the DUCT and the MARC-CDC programs. Again the calculations are in close agreement.

For the constant pressure case, the results by the DUCT program were obtained with 0.1 second computation time on a CDC 6600 computer. The results by the MARC-CDC program were obtained with 17 seconds computation time on a CDC 7600 computer. The computer times for the varying pressure case are approximately 0.4 and 17 seconds with DUCT and MARC-CDC program respectively. Because of its economic advantage, the DUCT program was used to generate a series of design curves.

4. DUCT DESIGN CURVES

In the FTR core during steady state operation, temperature of the coolant varies approximately from 644K (700°F) at the inlet to 811K (1000°F) at the outlet. Fast neutron flux has approximate cosine radial and axial distributions in the fuel region, the maximum being 4.5×10^{15} n/cm^2-sec, and the minimum, 2.5×10^{15} n/cm^2-sec. Pressure differential across the duct wall varies almost linearly from .014 MPa (2 psi) at the top of the assembly to .483 MPa (70 psi) at the bottom of the assembly. Each assembly is subjected to a different combination of pressure, temperature, and neutron flux in its core location. For these conditions, a set of curves was generated relating dilation to the various geometric and loading parameters. The structural material was assumed to be 20% cold worked type 316 stainless steel.

Figure 5 relates dilation of the duct at the end of 3 operating cycles (7200 hrs) at 741K (875°F) and 4.5×10^{15} n/cm^2-sec to the wall thickness and internal pressure. The abscissa is nondimensionalized with respect to the wall thickness (h), and the ordinate, the half width of the duct flat (L). As long as the dimensionless ratio, h/L is the same, the dilation characteristic shown in Figure 5 will hold regardless of the size of the duct. As expected, dilation decreases with thickness and increases with internal pressure.

Figure 6 shows the calculated dilation of a FTR duct at 741K (875°F) and 4.5×10^{15} n/cm^2-sec as a function of time and pressure differential. If it is assumed that duct-to-duct touching, w = .20 cm (.0775"), is the duct life limiting factor, the duct will reach its design life at 6300 hrs for p = .483 MPa (70 psi), at 8200 hrs for p = .221 MPa (32 psi), and at 11600 hrs for p = .014 MPa (2 psi). With a set of graphs such as those in Figure 6 at different temperatures and fluxes, dilation lifetime of the duct at different temperatures, pressures and fluxes can be determined. Figure 7 shows the variation of the duct dilation lifetime as a function of temperature and pressure with the flux at 4.5×10^{15} n/cm^{2}sec. Similar figures can be obtained for other flux levels. For the FTR duct in Row 1 at the core midplane, the temperature, pressure, and flux values are 741K (875°F), .221 MPa (32 psi) and 4.5×10^{15} n/cm^2/sec. According to Figure 7, it has a dilation lifetime of 3-1/2 cycles (8400 hrs.). Other combinations of temperature, pressure and flux have been examined. Considering only dilation, the lifetime of the FTR duct is predicted to be at least 3 cycles (7200 hrs) with the material laws used.

5. CONCLUSIONS

On the basis of the results presented in this paper, the following conclusions are drawn:

1. For conditions where there is very little stress redistribution, the method presented in this paper for solving the duct dilation problem is valid and requires minimal computer running time.
2. Under pressure differential, temperature and fast neutron flux, the hexagonal duct dilates in the following manner:
   a. the maximum dilation occurs at the mid-flat of the duct,
   b. the maximum stress and accumulated inelastic strain occur at the inside corner of the duct,
   c. dilation decreases with thickness and increases with duct size,
   d. dilation increases with temperature, internal pressure, fast neutron flux and irradiation time.

3. For the material laws assumed, the neighboring FTR ducts will not touch each other (except at the load pads) due to dilation alone in their intended length of service.

REFERENCES

1 "MARC-CDC Nonlinear Finite Element Analysis Program," Rev. G, Control Data Corp., Minneapolis, Minnesota, 1975.

2 Gilbert, E. R. and Blackburn, L. D., "Creep Deformation of 20% Cold Worked Type 316 Stainless Steel", Journal of Engineering Materials and Technology, Volume 99, April 1977, pp. 168-180.

3 Bates, John F., "An Empirical Relationship for Swelling in 20% Cold Worked Stainless Steel," HEDL-TME 76-96, March 1977.

NOMENCLATURE

E	-	Young's modulus
F	-	Axial force
h	-	Thickness of duct
I	-	Section modulus
L	-	Half of corner to corner distance along flat surface
M	-	Bending moment
n	-	Subscript denotes the quantity at time step n
p	-	Internal pressure
T	-	Uniform temperature
t	-	Time
u	-	Displacement in x direction
V	-	Shear force
v	-	Displacement in y direction
w	-	Displacement in z direction
X,Z	-	Coordinate directions in beam model, Figure 1
x	-	Distance along duct wall
z	-	Distance from centroid of the duct wall
ϕ	-	Neutron flux
α	-	Coefficient of thermal expansion
ε	-	Total strain
$\Delta\varepsilon^S$	-	Irradiation swelling strain increment
$\Delta\varepsilon^C$	-	Irradiation creep strain increment
σ	-	Axial stress

TABLE 1

COMPARISON OF DUCT AND MARC-CDC RESULTS
WITH PRESSURE VARIATION

Time Hrs	Corner Stress MPa (ksi) DUCT	Corner Stress MPa (ksi) MARC	Corner Strain % DUCT	Corner Strain % MARC	Mid Flat Dilation cm (in.) DUCT	Mid Flat Dilation cm (in.) MARC
0	54.66 (7.93)	55.57 (8.06)	0	0	0.053 (0.021)	0.053 (0.021)
3600	57.90 (8.40)	58.47 (8.48)	0.35	0.34	0.080 (0.032)	0.083 (0.033)
4200	66.38 (9.63)	67.02 (9.72)	0.44	0.43	0.090 (0.036)	0.093 (0.037)
4800	74.67 (10.83)	75.29 (10.92)	0.55	0.53	0.107 (0.042)	0.110 (0.043)
5400	82.74 (12.00)	83.29 (12.08)	0.69	0.66	0.128 (0.050)	0.131 (0.052)
6000	90.46 (13.12)	90.80 (13.17)	0.84	0.81	0.152 (0.060)	0.156 (0.061)
6600	97.97 (14.21)	98.11 (14.23)	1.01	0.97	0.177 (0.070)	0.181 (0.071)
7200	100.94 (14.64)	100.87 (14.63)	1.21	1.16	0.203 (0.080)	0.208 (0.082)

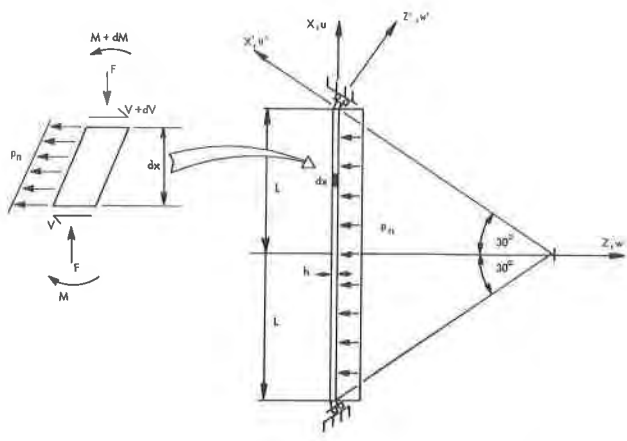

Figure 1. Mathematical model of 1/6th of a hexagonal duct.

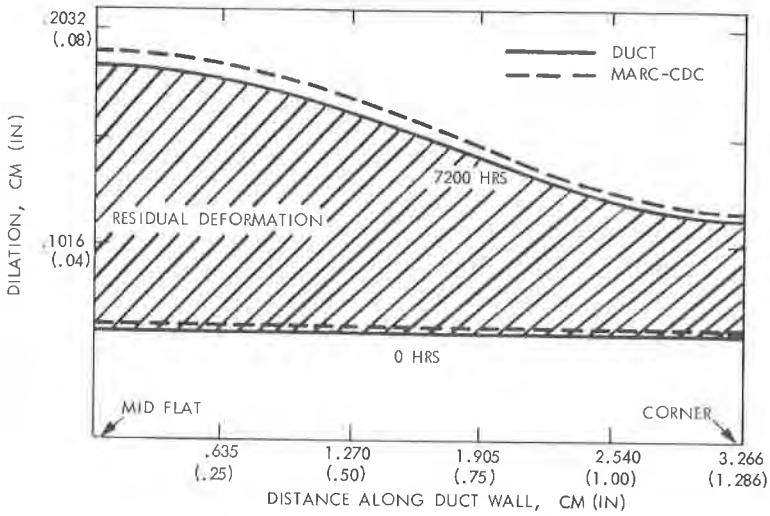

Figure 2. Dilation along the duct wall.

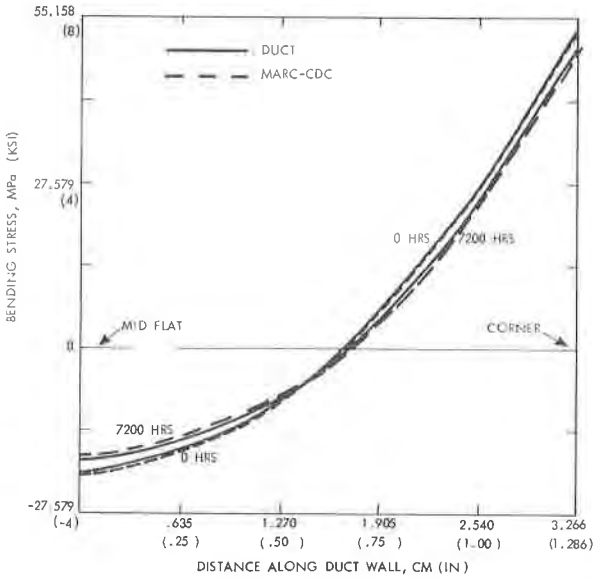

Figure 3. Bending stress along the inside surface of the duct wall.

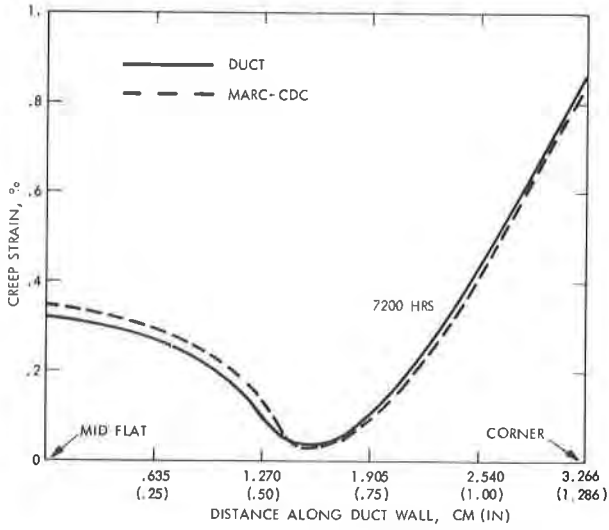

Figure 4. Creep strain along the inside surface of the duct.

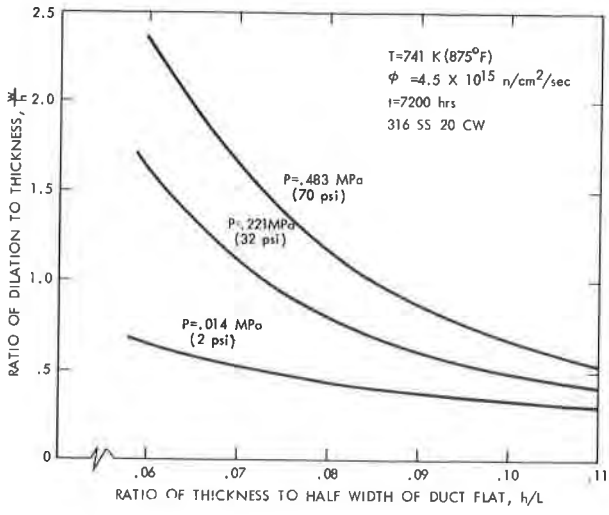

Figure 5. Variation of dilation with thickness and internal pressure.

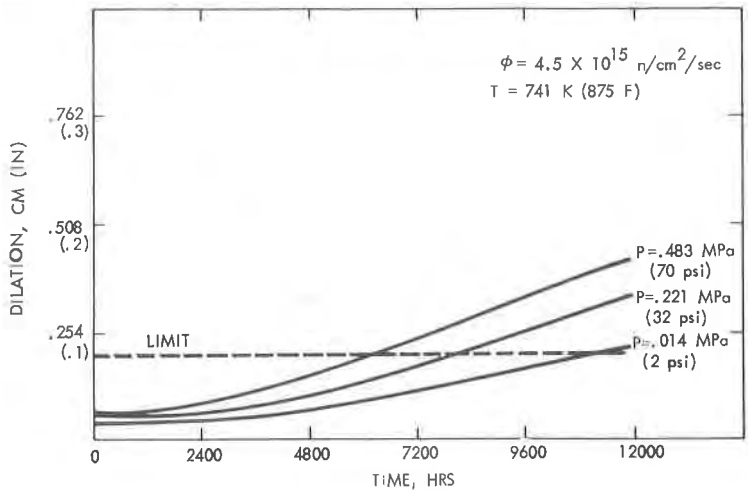

Figure 6. Dilation histories at different internal pressures.

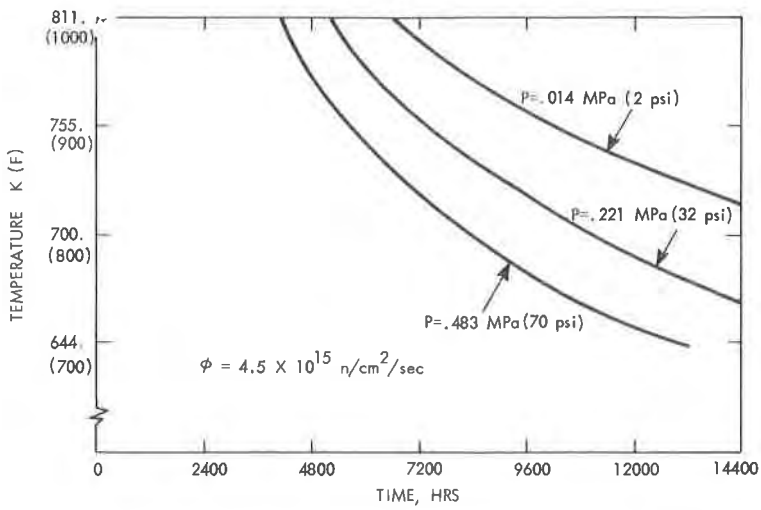

Figure 7. Lifetime of duct at different temperatures and pressures.